Chinese J. Chem. Eng., **14**(5) 604—610 (2006)

Analysis and Measurement of Mass Transfer in Airlift Loop Reactors*

ZHANG Tongwang(张同旺)**, WANG Tiefeng**(王铁峰) **and WANG Jinfu**(王金福)**
Beijing Key Lab of Reaction Engineering & Technology, Tsinghua University, Beijing 100084, China

Abstract Inter-phase mass transfer is important to the design and performance of airlift loop reactors for either chemical or biochemical applications, and a good measurement technique is crucial for studying mass transfer in multiphase systems. According to the model of macro-scale mass transfer in airlift loop reactors, it was proved that the airlift loop reactor can be regarded as a continuous stirred tank reactor for measuring mass transfer coefficient. The calculated mass transfer coefficient on such a basis is different from the volumetric mass transfer coefficient in the macro-scale model and the difference is discussed. To describe the time delay of the probe response to the change of oxygen concentration in the liquid phase, a model taking into account the time constant of response is established. Sensitivity analysis shows that this model can be used to measure the volumetric mass transfer coefficient. Applying this model to the measurement of volumetric mass transfer coefficient in the loop reactor, results that coincide with the turbulence theory in the literate were obtained.
Keywords airlift loop reactor, mass transfer model, sensitivity analysis

1 INTRODUCTION

Airlift loop reactors have emerged as one of the most promising devices in chemical, biochemical and environmental engineering operations. Its main advantages over conventional reactors include excellent contact among different phases, ease of removal or replenishment of particles, and high heat and mass transfer rates[1]. High gas-liquid contacting area and favorable flow pattern are the attractive features of this type of three-phase contactors. Typical processes that can use this type of reactors include synthesis of methanol or dimethyl ether from syngas, coal liquefaction, Fischer-Tropsch synthesis, petroleum refining, and wastewater treatment[2,3].

For the optimum design and operation of an airlift loop reactor, it is important to describe the mass transfer characteristics[4,5]. Meanwhile, theoretical studies on modeling the liquid-side mass transfer are necessary parts for the process design and evaluation. Recently, the shortage of the classical mass transfer theory has been undergoing the unceasing modification and improvement[6,7].

Although mass transfer characteristics have been investigated extensively, most researchers paid attention to the influence of operating conditions on volumetric mass transfer coefficient and the establishment of its model[8—10], but few of them focused on the measurement of the mass transfer coefficient. They considered the airlift loop reactor as a continuous stirred tank reactor (CSTR) without verification[11,12]. In this paper, it was proved that the airlift loop reactor can be regarded as a continuous stirred tank reactor when measuring volumetric mass transfer coefficient, even though the macro-scale mass transfer model is established based on plug flow. Because the volume concerned in the macro-scale model and that in the CSTR assumption are different, the calculated volumetric mass transfer coefficient based on the CSTR assumption is different from the volumetric mass transfer coefficient in the macro-scale mass transfer model. By taking into account the probe response time, a model was established for volumetric mass transfer coefficient calculation of airlift loop reactor. Sensitivity analysis shows that the volumetric mass transfer coefficient can be calculated precisely. By applying this model to the calculation of volumetric mass transfer coefficient in an airlift loop reactor, results that coincide with the turbulence theory in the literate were obtained[13].

2 MODEL

The liquid flow in the riser and down-comer can be considered to be plug flow. The influence of the mixing zones at the separator and the bottom junction are neglected and all these parts are considered to yield, together with the down-comer a pure delay τ_d, of the liquid. In this paper, air is considered as gas phase. The oxygen mole fraction variation of the gas flowing through the riser is considered to be negligible. The static pressure effect on gas concentration is taken into consideration[7].

Equation (1) is the oxygen balance equation in the riser. $k_L a_r$ is volumetric mass transfer coefficient of the riser which is the product of the mass transfer coefficient k_L and the special interfacial area a_r. ε is gas holdup in the riser and u_L is the liquid velocity in the

Received 2005-08-02, accepted 2006-02-27.
* Supported by the Specialized Research Fund for the Program of Higher Education (No.20050003030) and by Tsinghua-Zhongda Postdoctoral Fellowship Program (No.20283600131).
** To whom correspondence should be addressed. E-mail: wangjf@flotu.org

riser. A_{gl} is the gas-liquid inter-phase area and V_r is the volume of the riser. Here the effects of superficial gas velocity u_g and gas holdup ε are contained in the volumetric mass transfer coefficient. They influence the inter-phase mass transfer by changing the volumetric mass transfer coefficient. The oxygen concentration in liquid phase C_L is a function of axial position and time.

$$\frac{\partial C_L}{\partial t}+u_L\frac{\partial C_L}{\partial x}=k\left(\frac{C_G}{H}-C_L\right) \tag{1}$$

$$k=\frac{k_L a_r}{1-\varepsilon},\quad a_r=\frac{A_{gl}}{V_r}$$

Equation (2) is the recirculation condition. The concentration at the top of the riser is the concentration at the bottom of the riser after a delay τ_d.

$$C_L(0,t+\tau_d)=C_L(h,t) \tag{2}$$

Equation (3) is the initial condition that the liquid phase oxygen concentration is zero.

$$C_L(x,0)=0 \tag{3}$$

The bottom column pressure is taken as the reference. C_G^0 is oxygen concentration in gas phase at the bottom column. When the variation of the oxygen mole fraction in the gas phase is neglected, the gas phase oxygen concentration becomes proportional to the static pressure.

$$b=\frac{1-p(h)/p(0)}{h}$$

$$C_G(x)=C_G^0(1-bx)\quad C_L^0=\frac{C_G^0}{H} \tag{4}$$

By coordinate transformation between Eulerian coordinate and Lagrange coordinate, the analytical of the previous model can be obtained as follows[14].

$$C_L(0,t)=C_L^0-C_L^0bh+\frac{C_L^0bu_L}{k}+\left[C_L\left(0,t-\frac{h}{u_L}-\tau_d\right)-C_L^0-\frac{C_L^0bu_L}{k}\right]\exp\left(-k\frac{h}{u_L}\right) \tag{5}$$

$$C_L(0,t)=\begin{cases}0, & t\leqslant\dfrac{h}{u_G}+\tau_d\\ C_L^0\left[1-\exp\left(\dfrac{u_G(t-\tau_d)-h}{u_G-u_L}k\right)\right], & \dfrac{h}{u_G}+\tau_d<t\leqslant\dfrac{h}{u_L}+\tau_d\end{cases} \tag{6}$$

$$C_L(x,t)=C_L^0-C_L^0bx+\frac{C_L^0bu_L}{k}+\left[C_L\left(0,t-\frac{x}{u_L}\right)-C_L^0-\frac{C_L^0bu_L}{k}\right]\exp\left(-k\frac{x}{u_L}\right) \tag{7}$$

This is a recursion solution. The interfacial mass transfer rate depends not only on the volumetric mass transfer coefficient, but also on the specific interfacial area. The solute concentration at the entrance of the riser can be determined from Eqs.(5) and (6), then the evolution of the solute concentration at any other axial positions can be determined from Eqs.(5) and (7). Eqs.(5) to (7) show that the liquid velocity, u_L, and time delay, τ_d, have a great influence on the evolution of the solute concentration.

The parameters of the macro-scale oxygen mass transfer model are shown in Table 1. The influence of the liquid velocity, u_L, and time delay, τ_d, on the evolution of the solute concentration is investigated for an airlift loop reactor. The parameters in the model could be measured by experiment and were in the range of literature. Here is a hypothetical experiment. The values of these parameters have no influence on the staircase increase of the dissolved oxygen curve and the following conclusions.

Table 1 Parameters in the model of oxygen mass transfer

h, m	H, $m^3\cdot mol^{-1}$	T, K	U_{slip}, $m\cdot s^{-1}$	C_G^0, $mol\cdot m^{-3}$	k_La_r, s^{-1}
4.0	1.82×10^6	298.15	0.25	9.57	0.1

For certain volumetric mass transfer coefficient and time delay in the down-comer, Fig.1 shows the evolution of the oxygen concentration in the liquid phase under different liquid velocity u_L. Superficial gas velocity and gas holdup are not given in Fig.1, for the effect of superficial gas velocity and gas holdup on mass transfer by changing the special interfacial area has been contained in the volumetric mass transfer coefficient. With time evolving, the oxygen concentrations approach the same limit. However, the step change in the evolution of the oxygen concentration becomes gradually smaller with increasing liquid velocity. The evolution of the oxygen concentration shows approximately an exponential increase with increasing liquid velocity, indicating that the airlift loop reactor may be regarded as a continuous stirred tank reactor (CSTR) at large liquid velocity. The mass transfer equation in CSTR is shown as follows[15]:

$$\frac{dC_L}{dt}=k_La_w\left(\frac{C_G^*}{H}-C_L\right),C_L(0)=0 \tag{8}$$

where C_L is the oxygen concentration in the liquid phases, and C_G^* is the oxygen saturated concentration in the gas phases. The solution of Eq.(8) is:

$$\frac{C_L}{C_L^*}=1-\exp(-k_La_wt),\quad C_L^*=\frac{C_G^*}{H} \tag{9}$$

An equivalent form of Eq.(9) is

$$-\ln\left(1-\frac{C_L}{C_L^*}\right)=k_La_wt \tag{10}$$

Eq.(10) is linear, and the volumetric mass transfer coefficient is the slope. This shows that if the data obtained from Eqs.(5) to (7) can be described by Eq.(10) approximately, the assumption that the airlift loop reactor is CSTR would be reasonable.

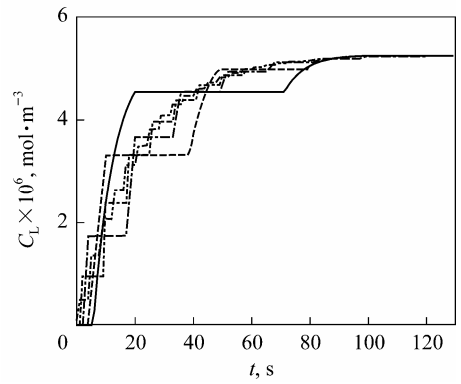

Figure 1 The evolution of oxygen concentration in the model at different liquid velocities
(k_La_r=0.1s^{-1}, τ_d=4s)
u_L, m·s^{-1}: —— 0.1; ----- 0.2; —·— 0.5; —·—·— 1.0; —··— 2.0

The data in Fig.1 after transformed according to Eq.(10) are shown in Fig.2. The logarithmic transformed curves are still step lines, but their slopes obtained from the least square approximation are equal. This indicates that the airlift loop reactor can be regarded as CSTR for mass transfer measurement, even though the macro-scale mass transfer model is established based on a plug flow assumption. This is because the liquid recirculation leads to global mixing in airlift loop reactors, and the CSTR assumption can be used to calculate the volumetric mass transfer coefficient. However, the calculated mass transfer coefficient based on CSTR assumption is not the volumetric mass transfer coefficient in the macro-scale mass transfer model of Eqs.(5) to (7). The relationship between these two volumetric mass transfer coefficients will be discussed in the following section.

The other important parameter in the macro-scale mass transfer model is the time delay, τ_d, in the down-comer. Fig.3 shows the evolution of the oxygen concentration under different τ_d. The profiles of the oxygen concentration are different under different τ_d, even though the volumetric mass transfer coefficients in the macro-scale model were the same value. According to Eq.(10), the data in Fig.3 were transformed and shown in Fig.4. Three different slopes can be obtained by using the least square method. This shows that τ_d has influence on the volumetric mass transfer coefficient calculated from the concentration curve based on CSTR assumption. According to the physical meaning of the time delay, larger time delay means larger volume of the down-comer. There is no inter-phase mass transfer in the down-comer, while the CSTR assumption means that there is inter-phase mass transfer everywhere. Because the volume concerned in the macro-scale model is the liquid volume in the riser, while the volume concerned in the CSTR is the liquid volume in the whole reactor, the specific interfacial area, a_r, in the macro-scale model is different from the specific interfacial area, a_w, in the CSTR assumption.

$$a_r=\frac{A_{GL}}{V_r},\qquad a_w=\frac{A_{GL}}{V_r+V_d} \tag{11}$$

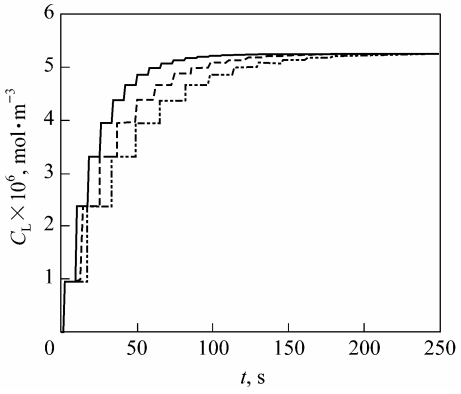

Figure 3 The evolution of oxygen concentration in the model under different time delay
(k_La_r=0.1s^{-1}, u_L=1m·s^{-1})
τ_d, s: ——4; ----- 8; —··— 12

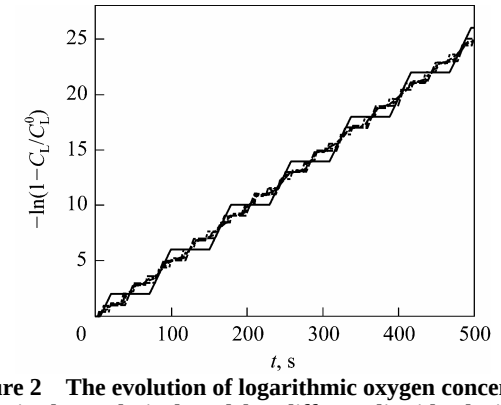

Figure 2 The evolution of logarithmic oxygen concentration in the analytical model at different liquid velocities
(k_La_r=0.1s^{-1}, τ_d=4s)
u_L, m·s^{-1}: ——0.1; ----- 0.2; —·— 0.5; —·—·— 1.0; —··—2.0

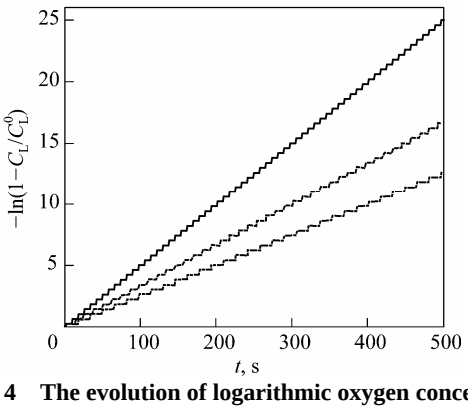

Figure 4 The evolution of logarithmic oxygen concentration in analytical model under different time delay
(k_La_r=0.1s^{-1}, u_L=1m·s^{-1})
τ_d, s: ——4; ----- 8; —··— 12

Because the liquid flux in the riser is equal to the liquid flux in the downer, a_r and a_w are subject to the following equation:

$$\frac{a_r}{a_w}=\frac{V_r}{V_r+V_d}=\frac{\tau_r}{\tau_r+\tau_d} \tag{12}$$

So the calculated mass transfer coefficient based on the CSTR assumption, k_La_w, and the mass transfer coefficient in the macro-scale model, k_La_r, has the following relationship:

$$\frac{k_La_w}{k_La_r}=\frac{\tau_r}{\tau_d+\tau_r} \tag{13}$$

Figure 5 compares the volumetric mass transfer coefficient in the macro-scale model, k_La_r, and the calculated mass transfer coefficients based on CSTR assumption, k_La_w, under different time delays. The ratios of k_La_r to k_La_w are the same value under the same time delay in the down-comer, τ_d. Fig.6 compares k_La_r and the modified k_La_w by using Eq.(13). All the points are on the diagonal, showing that the airlift loop reactor can be assumed as CSTR for calculating mass transfer coefficient. With the consideration that the volumetric mass transfer coefficient discussed in the literatures[2,6,11] were all based on the liquid volume in the whole reactor, we also pay our attention to the volumetric mass transfer coefficient calculated from CSTR assumption in the following discussions.

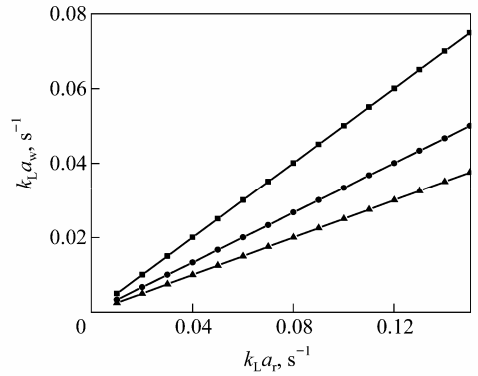

Figure 5 Comparison between k_La_r and k_La_w under different time delays

τ_D, s: ■ 4; ● 8; ▲ 12

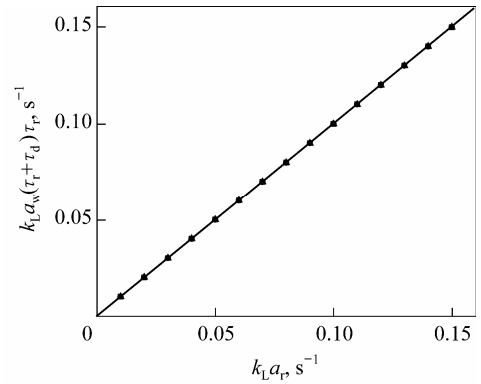

Figure 6 Comparison between k_La_r and amended k_La_w under different time delays

τ_D, s: ■ 4; ● 8; ▲ 12

Galvanic oxygen sensor probe was frequently used to measure the oxygen concentration in the liquid phase[16,17]. Due to response delay of the sensor probe, the change of the oxygen concentration in the liquid phase cannot be instantaneously detected. For galvanic oxygen sensors, the real oxygen concentration and the response of the sensor probe have the following relation:

$$\frac{dC_m}{dt}=k_p(C_L-C_m),\quad C_m(0)=0 \tag{14}$$

where C_m is the oxygen concentration measured by the sensor. The following equation can be obtained from Eqs.(8) and (14):

$$\frac{d^2C_m}{dt^2}+(k_p+k_La_w)\frac{dC_m}{dt}+k_pk_La_wC_m-k_pk_La_w\frac{C_G^*}{H}=0 \tag{15}$$

The initial condition is:

$$C_m(0)=0,\quad C_m^{(1)}(0)=0 \tag{16}$$

The solution to Eq.(15) and Eq.(16) is:

$$\frac{C_L^*-C_m(t)}{C_L^*-C_m(0)}=\frac{1}{k_p-k_La_w}\left[k_p\exp(-k_La_wt)-k_La_w\exp(-k_pt)\right] \tag{17}$$

Eq.(17) shows the relationship between the oxygen concentration in the liquid phase and the measured value.

3 EXPERIMENTAL

To validate the proposed model, Eq.(17), experiments were carried out in an airlift external-loop reactor with a height of 3.2m, as shown in Fig.7. The diameter of the riser and down-comer are 100mm. Tap water was used as the liquid phase. The gas feed could be switched from air to nitrogen or *vice versa*. Water

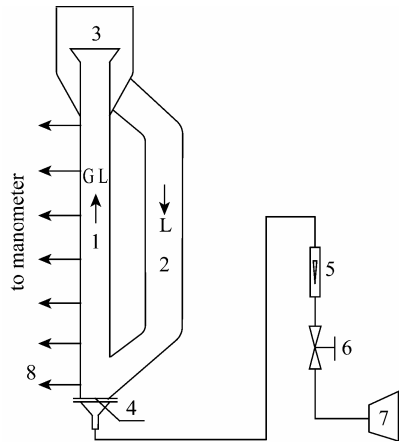

Figure 7 The schematic diagram of the experimental apparatus

1—riser; 2—downcomer; 3—gas-liquid separator; 4—gas distributor; 5—flow meter; 6—valve; 7—compressor; 8—manometer

was de-oxygenated by stripping with nitrogen, with a rapid switchover after de-oxygenated from the nitrogen stream to an air stream. The oxygen sensor probe was mounted at 2.8m above the gas distributor in the riser. The signal obtained by the sensor probe was stored in a PC and the sample frequency is 10Hz. In order to verify the model in a wider operating condition, FCC catalyst was used as solid phases to investigate the volumetric mass transfer coefficient in gas-liquid-solid three-phase system. The average diameter and density of the solid particles are 60μm and 2176.8kg·m^{-3}, respectively. The solid holdup has reached 20% (by volume).

The experimental sensor response coefficient, k_p, was measured by a classical concentration switch method. The sensor probe was dipped into water of low oxygen concentration by bubbling nitrogen. When the signal was stable, the sensor probe was dipped into water of high oxygen concentration by bubbling air. The response was shown in Fig.8, and k_p was determined to be 0.105s^{-1} according to Eq.(14). Because there was a liquid layer out of the sensor probe, the measured probe response coefficient was determined by the sensor probe and the liquid layer out of the probe.

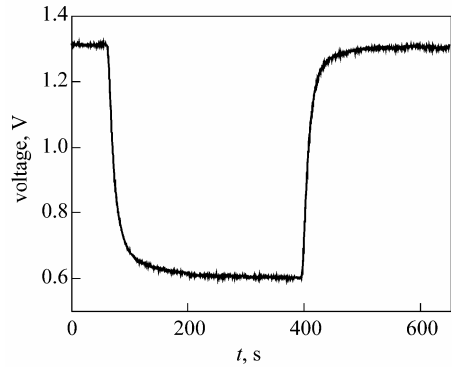

Figure 8 The response of the oxygen sensor to step change of oxygen concentration

In the airlift loop reactor, the liquid moved directionally. The liquid layer out of the sensor probe was different from that when measuring the probe response coefficient. It was made that there might be some difference between the probe response coefficient in the airlift loop reactor and the measured probe response coefficient.

Equation (17) contains two parameters, namely the volumetric mass transfer coefficient, k_La_w, and the probe response coefficient, k_p. Because of the presence of k_p, k_La_w cannot be directly obtained from Eq.(10) by using the least square method[18]. Their effects were studied by analyzing the sensitivity of Eq.(17) to the variations around the optimum of the objective function[19,20]. The objective function according to which the parameters were estimated was the least square residual, R, of the experimental data and the predicted value calculated by Eq.(17). The R value was calculated by the following expression:

$$R=\left(\frac{\int_0^{\infty}\left[C_{\exp}(t)-C_{\mathrm{cal}}(t)\right]^2\mathrm{d}t}{\int_0^{\infty}\left[C_{\exp}(t)\right]^2\mathrm{d}t}\right)^{1/2} \tag{18}$$

$C_{\exp}(t)$ is the experimental concentration and $C_{\mathrm{cal}}(t)$ is the calculated concentration for certain k_La_w and k_p. The closer the R value approaches 0, the more perfect the fit is. k_La_w and k_p that made R the least are the volumetric mass transfer coefficient of the reactor and the probe response coefficient. The contour lines with varying parameters intervals for the R values of the fit were plotted in Fig.9. It shows that the identifiability of the two parameters is good, and the determination of the mass transfer coefficient is more precise than that of the probe response coefficient. The sensitivity analysis can be used to calculate the volumetric mass transfer coefficient and probe response coefficient according to the curve of the experimental oxygen concentration.

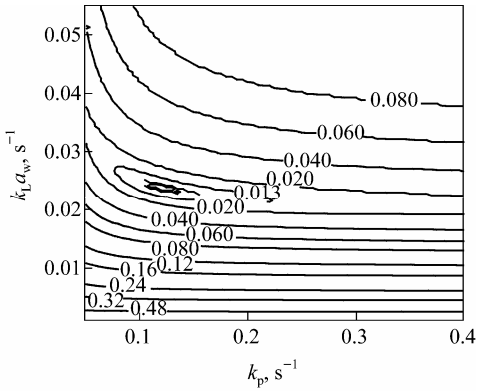

Figure 9 Sensitivity of the model to k_La_w and k_p variations in airlift loop reactors
(C_S=0, U_G=0.1133m·s^{-1})

Figure 10 compares the experimental data and predication calculated with sensitivity analysis under different operating conditions, showing good agreement. Fig.11 shows the probe response coefficients with increasing superficial gas velocity under different operating conditions. Because the objective function is not as sensitive to the probe response coefficient as to the volumetric mass transfer coefficient, the probe response coefficient varies irregularly. However, it fluctuates at 0.125s^{-1} and it was used for the probe response coefficient. This value is different from the previous value, 0.105s^{-1}, obtained from the classical concentration switch method. This is because the water was static when using the classical concentration switch method, while the water flows directionally in the loop reactor. The water flow tenuates the liquid layer out of the sensor probe and make the sensor probe response coefficient increase.

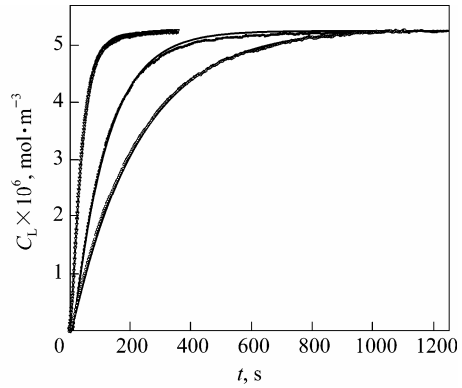

Figure 10 Comparison between the experimental data and the model (C_S=0.05)
U_G, m·s^{-1}: ○ 0.0283; ■ 0.092; ▽ 0.1558

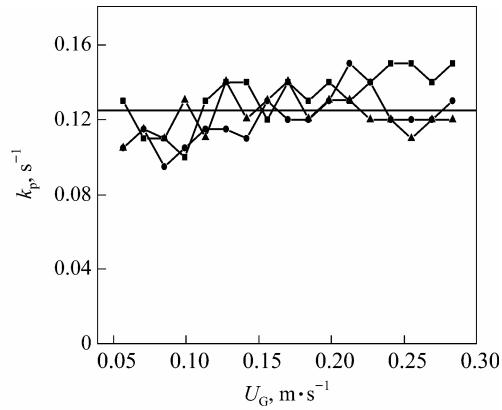

Figure 11 The sensor response coefficient under different solid loadings
C_S: ■ 0; ● 0.01; ▲ 0.05

Figure 12 shows the volumetric mass transfer coefficients, k_La_w, under different solid loadings. k_La_w decreases with increasing solid loading, similar to that obtained in the literature[21]. The addition of solid enhances bubble coalescence and decreases the gas holdup, which in turn decrease the interfacial area and volumetric mass transfer coefficient. k_La_w shows an approximately linear increase with increasing superficial gas velocity. The trend coincided with the turbulence theory in the literature[13].

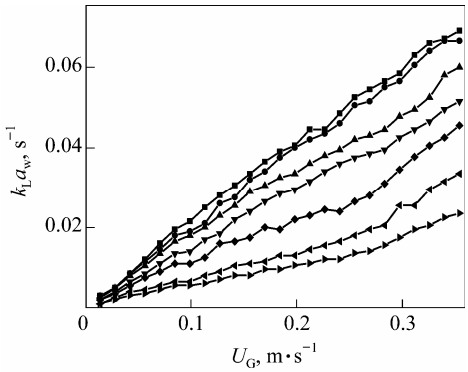

Figure 12 The mass transfer coefficient under different solid loadings
C_S: ■ 0; ● 0.025; ▲ 0.05; ▼ 0.075; ◆ 0.1; ◄ 0.15; ► 0.2

4 CONCLUSIONS

According to the macro-scale mass transfer model of the airlift loop reactor, it was proved that the airlift loop reactor can be regarded as a continuous stirred tank reactor for measuring mass transfer coefficient. The global mixing during oxygen mass transfer in an airlift loop reactor was mainly due to liquid recirculation. Because of the difference between the volumes concerned in the macro-scale model and that in the CSTR model, the calculated mass transfer coefficient based on CSTR assumption was different from the volumetric mass transfer coefficient in the macro-scale model. Because the probe cannot instantaneously respond to the change of oxygen concentration in the liquid phase, the measured value was not the real oxygen concentration in reactor. In order to obtain the accurate volumetric mass transfer coefficient, a model that took into account the probe response coefficient was established. Sensitivity analysis was applied to the model, showing that this model can be used to calculate the volumetric mass transfer coefficient and the probe response coefficient. The probe response coefficient obtained from the sensitivity analysis was larger than that obtained from the classical concentration switch method. This is because water moves directionally in the reactor and makes the liquid layer out of the probe thinner. Appling the proposed model to the measurement of volumetric mass transfer in an airlift loop reactor, the regularity coincided with the turbulence theory in the literature. This shows that the mass transfer coefficient measurement technique proposed in this paper is reasonable and practicable.

NOMENCLATURE

A	gas-liquid interfacial area, m^2
a	specific surface area, m^{-1}
C	oxygen concentration, mol·m^{-3}
C_S	solid volume fraction
H	Henry number, m^3·mol^{-1}
h	reactor height, m
k_La	volumetric mass transfer coefficient, s^{-1}
k_p	sensor response coefficient, s^{-1}
p	pressure, Pa
t	time in Lagrange coordinate, s
U	velocity, m.s^{-1}
V	volume, m^3
ε	gas holdup
τ	time delay, s

Subscripts

d	down-comer
G	gas
L	liquid
p	probe
r	riser
slip	slip velocity
w	whole reactor

REFERENCES

1 Siegel, M.H., Robinson, C.W., "Applications of airlift gas-liquid-solid reaction in biotechnology", *Chem. Eng.*

Sci., **47**(13/14), 3215—3229(1992).
2 Choi, K.H., Chisti, Y., Moo-Young, M., "Comparative evaluation of hydrodynamic and gas-liquid mass transfer characteristics in bubble column and airlift slurry reactors", *Chem. Eng. J*., **62**, 223—229(1996).
3 Yang, W.G., Wang, J.F., Jin, Y., "Gas-liquid mass transfer in a slurry bubble column reactor under high temperature and high pressure", *Chin. J. Chem. Eng*., **9**(3), 4—9(2001).
4 Siegel, M.H., Merchuk, J.C., "Mass transfer in a rectangular air-lift reactor: Effect of geometry and gas recirculation", *Biotechnol. Bioeng*., **32**(9), 1128—1137(1988).
5 Garcia-Ochoa, F., Gomez, E., "Theoretical prediction of gas-liquid mass transfer coefficient, specific area and hold-up spragered stirred tanks", *Chem. Eng. Sci*., **59**, 2489—2501(2004).
6 Wen, J.P., Jia, X.Q., Mao, G.Z., "Local liquid side mass transfer model in gas-liquid-solid three-phase flow airlift loop reactor for Newtonian and non-Newtonian fluids", *Chin. J. Chem. Eng*., **12**(3), 347—350(2004).
7 Dhaouadi, H., Poncin, S., Midoux, N., Wild, G., "Gas-liquid mass transfer in an airlift reactor-analytical solution and experimental confirmation", *Chem. Eng. Process*., **40**, 129—133(2001).
8 Kawase, Y., Hashiguchi, N., "Gas-liquid mass transfer in external-loop airlift columns with Newtonian and non-Newtonian fluids", *Chem. Eng. J*., **62**(1), 35—42(1996).
9 Guo, Y.X., Rathor, M.N., Ti, H.C., "Hydrodynamics and mass transfer studies in a novel external-loop airlift reactor", *Chem. Eng. J*., **67**, 205—214(1997).
10 Shimizu, K., Takada, S., Takahashi, T., Kawase, Y., "Phenomenological simulation model for gas hold-ups and volumetric mass transfer coefficients in external-loop airlift reactors ", *Chem. Eng. J*., **84**, 599—603(2001).
11 Chisti, M.Y., Airlift Bioreactors, Elsevier Applied Science, New York (1989).
12 Al-Masry, W.A., Dukkan, A.R., "The role of gas disengagement and surface active agents on hydrodynamic and mass transfer characteristics of airlift reactors", *Chem. Eng. J*., **65**, 263—271(1997).
13 Tobajas, M., Garcia-Calvo, E., Siegel, M. H., Apitz, S.E., "Hydrodynamics and mass transfer prediction in a three-phase airlift reactor for marine sediment biotreatment", *Chem. Eng. Sci*., **54**(1), 5347—5354(1999).
14 Zhang, T.W., Zhao, B., Wang, J.F., "Mathematical models for macro-scale mass transfer in airlift loop reactors", *Chem. Eng. J*., **119**(1), 19—26(2006).
15 Levenspiel, O., Chemical Reaction Engineering, Wiley, New York (1999).
16 Luo, R.X., Li, Y.X., Chen, A.F., "The investigation and fabrication of galvanic oxygen sensor", *Journal of Beijing Institute of Chemical Technology*, **21**(4), 71—79(1994). (in Chinese)
17 Li, G.Q., Yang, S.Z., Cai, Z.L., Chen, J.Y., "Mass transfer and hydrodynamics in an airlift reactor with viscous non-Newtonian fluid", *Chin. J. Chem. Eng*., **3**(1), 23—31(1995).
18 Van't Riet, K., "Review of measuring methods and results in nonviscous gas-liquid mass transfer in stirred vessels", *Ind. Eng. Chem. Proc. Des. Dev*., **18**(3), 357—364(1979).
19 Korpijarvi, J., Oinas, P., Reunanen, J., "Hydrodynamics and mass transfer in an airlift reactor", *Chem. Eng. Sci*., **54**(13/14), 2255—2262(1999).
20 Dhaouadi, H., Poncin, S., Hornut, J. M., Wild, G., Oinas, P., "Hydrodynamics of an airlift reactor: Experiments and modeling", *Chem. Eng. Sci*., **51**(11), 2625—2630(1996).
21 Freitas, C., Teixeira, J.A., "Oxygen mass transfer in a high solids loading three-phase internal-loop airlift reactor", *Chem. Eng. J*., **84**(1), 57—61(2001).